Modeling and Design of a Microfluidic Respirometer for Continuous Amperometric Short Time Biochemical Oxygen Demand (BOD_{st}) Analysis

Albert Torrents[a], Jordi Mas[b], Francesc Xavier Muñoz[a], Francisco Javier del Campo[a]*

[a] Institut de Microelectrònica de Barcelona, IMB-CNM (CSIC)
[b] Universitat Autònoma de Barcelona Departement de Genètica i Microbiologia
* Campus Universitat Autónoma de Barcelona s/n Cerdanyola del Vallès (Barcelona, Spain).
javier.delcampo@csic.es

Abstract: This paper presents the design of a miniaturized electrochemical respirometer to monitor organic content in water samples semi-continuously, in contrast to current Biochemical Oxygen Demand, BOD, methods. We demonstrate the use of finite element method simulations as design tool for a novel concept microfluidic respirometer. The device is based on a flow cell separated by a thin membrane from a bioreactor. Simulations show that once membrane material and thickness are chosen, oxygen supply rate still provides sufficient flexibility to allow the measurement of samples spanning a very wide range of organic matter concentrations. The design presented here uses an electrochemical oxygen sensor, and the whole system is amenable to fabrication using standard microfabrication and rapid prototyping techniques.

Keywords: Modeling, BOD biosensor, Respirometry, Electrochemistry, Microfluidics, Finite Element Method.

1. Introduction

This work focuses on the design of a novel miniaturized system for the continuous determination of BODst (short-time Biological Oxygen Demand) in aqueous samples. The determination of BOD consists on the oxidation of organic matter by living organisms. After an adaptation time the amount of oxygen consumed over a typical period of 5 days is determined. This long analysis time makes BOD_5 expensive and unsuitable for process control, and opens a window of opportunity to rapid methods [1]. Perhaps the first example of a rapid BOD sensor was presented in 1977 [2]. Karube et al. Karube's method was reportedly able to provide close BOD estimates within 1 hour.

The evolution of so-called rapid BOD methods has been recently reviewed by Ponomareva et al. [3]. This work describes the design of a miniaturized respirometer that combines some of the advantages of biofilm biosensors and bioreactor BOD sensors, aiming to provide BOD information within a few hours. This is possible thanks to miniaturization and microfluidics.

1.1 Device description

Broadly, our concept consists in a flow cell where two media separated by an oxygen permeable membrane run together, and different oxygen sensors placed before and after the membrane measure oxygen supply and consumption. An oxygen-saturated electrolyte flows through one of the channels, in which an oxygen sensor is placed downstream. The second channel is filled with a mixture of biomass and the sample to be analyzed. This biomass/sample mixture remains stagnant during the measurement, while a thin oxygen membrane allows the diffusion of oxygen from the electrolyte channel to it.

Electrolyte flow rate and membrane thickness control the transport of oxygen to the biomass chamber, where it is consumed. The electrolyte flowing in is saturated with oxygen. As the electrolyte flows through the channel, oxygen diffuses across a thin membrane towards the biomass chamber where it is consumed by the biomass in the presence of organic matter. This drop in oxygen concentration inside the electrolyte channel is measured amperometrically at the end of the channel, which provides direct information on the respiration rate of the biomass and tells whether the electrolyte flow rate is adequate

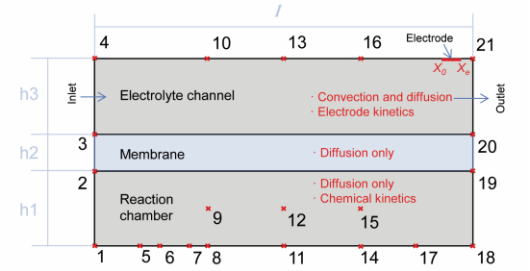

Figure 1: Schematic side-view diagram of the device (x and y axis are not at same scale). The scheme shows main subdomains and the physics applied at each subdomain. **L**: total lengt; **h1**: reaction chamber height; **h2**: membrane height; **h3**: Electrolyte channel height. See text and tables for further details.

2. Use of COMSOL Multiphysics

Figure 1 depicts a schematic draw of the subdomains, boundaries and modules used to solve the present model. Numbers in figures correspond to numbers specified in graphics.

2.1 Mathematical model

The respirometer model accounts for three fundamental phenomena, which are mass transport, respiration kinetics and electrode kinetics.

a) Mass transport

The modes of mass transport operating in our system are diffusion in the two chambers and the membrane, and convection by laminar flow in the electrolyte channel.

The laminar flow in the electrolyte channel is described by the Navier-Stokes equations for an incompressible Newtonian fluid:

$$\rho(u\nabla)u - \eta\nabla^2 u + \nabla p = 0$$
$$\nabla \cdot u = 0 \qquad (2)$$

Where ρ and η are the density and kinematic viscosity of the fluid, u is the velocity vector and p is pressure.

In addition, mass transport of dissolved species in the two chambers and in the membrane is described by:

$$\frac{\partial C_i}{\partial t} = -D_i\nabla^2 C_i + u\nabla C_i \qquad (3)$$

Where C_i and D_i are the concentration and diffusion coefficient of species i.

An additional reaction term, $-r_i$, needs to be added to the mass transport equation in the biomass chamber, to account for the consumption of oxygen and organics. This term is described in detail in the following section.

Transport of oxygen across the membrane is modeled using the approach described in previously published works. [4,5]

b) Respiration kinetics

Oxygen is consumed by bacteria as they metabolize aerobically the organic matter present in the sample. We are assuming that the medium can be considered homogeneous –no suspended solids- and a Michaelis-Menten-like mechanism where the bacteria first reach an equilibrium with the organic matter present and then take up oxygen to decompose that matter into CO_2 and water:

$$bacteria + organics \underset{k_{-1}}{\overset{k_1}{\rightleftharpoons}} bact\_org$$
$$bact\_org + O_2 \xrightarrow{k_2} bact + CO_2 + H_2O \qquad (4)$$

Where *bact* is the number of microbial cells without reduced organic matter in their cytosol, *organics* is the amount of organic matter as function of the oxygen required to be degraded, *bact_org* represents the microbial cells with reduced organic matter in its cytosol and k_1 and k_{-1} are the forward and backward reaction kinetic rates respectively. k_2 is the kinetic rate for respiration, treated as an irreversible process, and O_2 is the amount of oxygen present, CO_2 and H_2O are the final products of the reaction.

Although this is oversimplifying what really goes on in the process, it suffices for the purpose of our model, which is the design of a microsystem.

Applying the steady-state approximation to the above mechanism yields the following rate equations for oxygen and organics:

$$\frac{dO_2}{dt} = \frac{-k_1 k_2 Bact_0 \cdot Organics \cdot O_2}{k_{-1} + k_2 O_2 + k_1 Organics} \qquad (5)$$

And

$$\frac{dOrganics}{dt} = Bact_0 \cdot Organics\left\{\frac{\left[k_1\left(k_1 Organics + k_{-1}\right)\right]}{k_{-1} + k_2 O_2 + k_1 Organics} - k_1\right\} \qquad (6)$$

Where: $Bact_0$ is the initial concentration of bacteria.

c) Electrode kinetics

The last part in our model is the electrochemical detection of oxygen at an electrode. The overall reaction is:

$$O_2 + 4H^+ + 4e^- \rightarrow 2H_2O \qquad (7)$$

While equation 3 above describes mass transport of oxygen to the electrode, electron transfer is described by the Butler-Volmer equation and the current is calculated as:

$$I = nFD_{O_2} w \int_0^{x_e} \left. \frac{\partial O_2}{\partial y} \right|_{y=0} dx \qquad (8)$$

Were w represents electrode width, and x_e electrode length, respectively. F is the Faraday constant, and D_{O2} and n are the diffusion coefficient of oxygen and the number of electrons involved in the process.

Table 1 summarizes the values used for the different constants used in the simulations, and Table 2 summarizes the boundary conditions.

We followed a step-by-step approach to the simulation of this respirometer so that the main physical phenomena could be studied in isolation. First we looked at how oxygen crosses the membrane in an "infinitely" long respirometer. Next, we considered the consumption of oxygen at the biomass chamber and, last, we studied the best placement for the electrochemical oxygen sensor.

2.2 Meshing and accuracy

Meshing is crucial to Finite Element Methods (FEM) as it controls the accuracy of the results. [6] We are aware of the limitations of the method and have taken the steps to achieve results that are accurate to between 1% and 0.5% unless otherwise stated. Simulated currents were compared with those predicted by the Levich expression [7] for a microband inside a single microchannel.

In general, three model features forced us to work with a greater number of nodes, which increased the number of degrees of freedom in the simulations and the calculation requirements. The first was that the ratio between magnitudes in the x and y directions was about three orders of magnitude (l=13 cm versus 125 <h< 300 μm), which means that to avoid the propagation of significant errors along the simulation domains we needed to work with very fine elements over an extensive domain. Another important factor was the need to minimize the sources of error in the calculation of oxygen fluxes across the membrane domain, where particularly fine meshes were used. The third region where a fine mesh was mandatory was at the electrode-solution boundary, where a strong oxygen concentration gradient exists and the flux of oxygen towards the electrode needs to be calculated with high accuracy. Taking the previous considerations into account, meshes ranging from $14x10^4$ to over $45x10^4$ triangular elements, with a minimum element quality ranging from 0.78 to 0.84, and an average mesh quality ranging from 0.98 to 0.99 were used in the different models. [8]

Last, simulations were run in COMSOL multiphysics v.4.1 running on Linux OpenSuse on a SUN X2200 M2 workstation (64 Gb RAM at 2,2 GHz clock speed dual Quad Core AMD Opteron 2354).

2.3 Modeling and procedure

To solve the problem under study, we first have solved the laminar flow of the electrolyte channel using a stationary approach. We have used a direct MUMPS solver with a relative tolerance of $1 \cdot 10^{-5}$.

Then we have introduced the results of this stationary solution as input solution for the time dependent solver. Here a MUMPS solver with an absolute tolerance of $1 \cdot 10^{-7}$, time stepping using BDF method with maximum order 3 has been used to solve the mass transport and oxygen reaction in the electrolyte channel, membrane and reaction chamber subdomains.

The electrode response has been directly calculated at the electrode boundary and an integration considering the z axis has been established to calculate the overall current generated in the electrode.

3. Results and discussion

3.1 Oxygen transport

One key requirement of any respirometric device is that oxygen supply does not limit the respiration rate of the biomass. In our system this means that oxygen transport across the membrane separating electrolyte and biomass

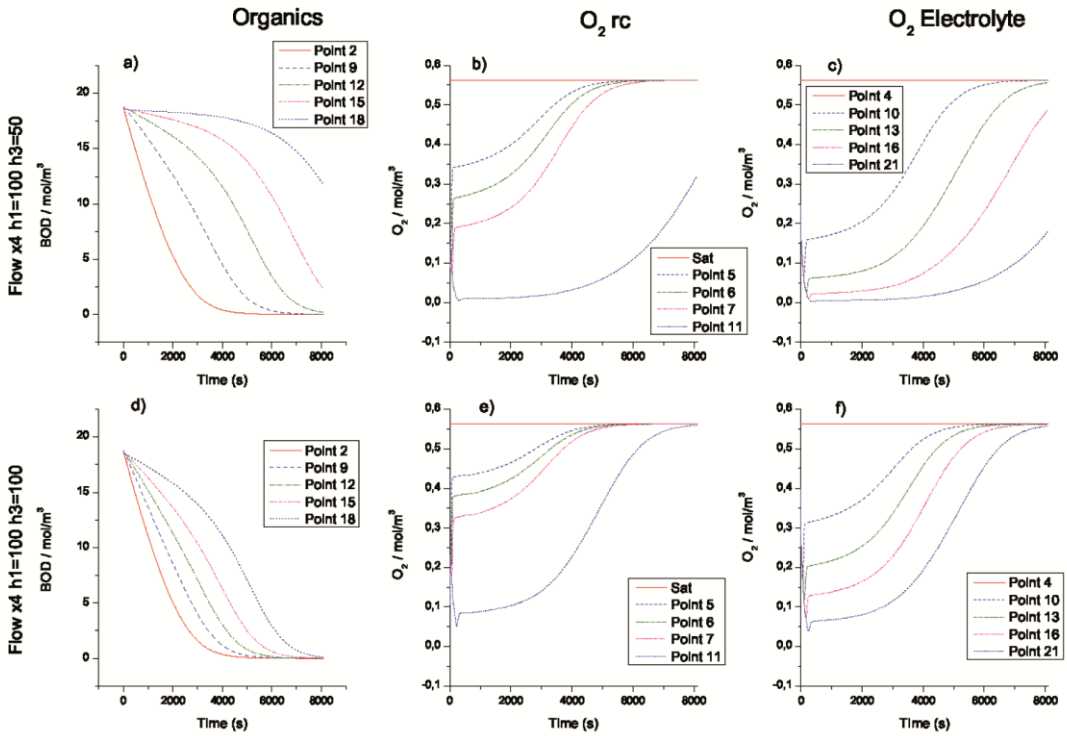

Fig. 2. Concentrations of organics and O2 at models with reaction, with modified channels heights. Concentrations of organics and O2 at models with reaction. The figure shows results for 300 mg/l (18,71 mole/m3) of BOD as initial loading of the device with flows of 0.60 _l min−1 and different h1 and h3. (a) and (d): concentration dynamics of BOD at reaction chamber; (b) and (e): concentration dynamics of O2 at reaction chamber; (c) and (f): concentration dynamics of O2 at electrolyte channel. See text for further details.

chambers is sufficiently fast to prevent the onset of anaerobic conditions in the biomass chamber. In this section we analyze data from the bottom of the biomass chamber because, as it is farthest from the membrane, it is where more limiting conditions may be found in a real system. Figure 1 shows a side-view diagram of the system where the various model features. The points highlighted show the locations where the concentrations of the different species were studied.

We studied three different thicknesses: 25, 75 and 200 microns. In this case the heights of the electrolyte and biomass chamber have been set equal to 100 microns, and the electrolyte flows with a linear velocity of 1 mm/s. These are all values that can be typically found in microfluidic devices. The effect of flow and respiration rates will be addressed separately.

To model the two materials, we played with their reported oxygen permeabilities and membrane thickness.

The higher permeability and the faster diffusion of oxygen displayed by PDMS membranes, brings about a fast drop in the oxygen concentration in the electrolyte channel until the biomass chamber fills up. Thus, the oxygen concentration profile advances at a similar velocity along the microchannel and inside the biomass chamber.

On the other hand, the lower oxygen diffusion rate across PTFE results in the biomass chamber gradually filling up more or less at the same rate everywhere, while oxygen is not significantly depleted anywhere in the electrolyte channel. In terms of membrane thickness, a set of three thicknesses that are either commercially available, have been chosen for the simulations: 25, 75 and 200 μm. The most obvious effect of increasing membrane thickness is the delay in diffusion time from the electrolyte channel into the biomass chamber. In fact, in the case of PTFE membranes, as membrane thickness increases beyond a certain limit, the oxygen concentration in the biomass chamber does not

reach the saturation level found in the electrolyte solution during the simulated time. PDMS membranes, on the other hand, see a response delay on increasing membrane thickness, but the oxygen supplied by the electrolyte eventually becomes fully available throughout the biomass chamber. In the next section, we study the behavior of this microrespirometric device when the biomass chamber contains a microbial population in contact with samples of different organic matter concentrations.

3.2 Respiration kinetics

In our model, the rate of respiration is a function of both oxygen and organic matter concentration available, as we consider a constant bacterial concentration set at 10^9 cfu mL^{-1}, and higher concentrations may be accessible when dealing with immobilized or highly agglomerated bacteria. The literature describes how the rate of organic matter degradation and, consequently, the rate of oxygen consumption, depend on the type and concentration of organic matter and on the type and growth (and so richness) of the microbial population, [1, 9, 10] so modulating the biomass concentration should provide some additional control over the respiration rate. On the other hand, having too high a concentration of bacteria may be counterproductive, as oxygen may be turned into a limiting factor regardless of electrolyte flow rate and oxygen concentration in it.

The three initial concentrations chosen for the organic matter correspond to three usual loadings found in real situations; a wastewater treatment plant discharge (30 ppm), typical urban waste water (300 ppm) and levels of 3000 ppm may be found in agricultural or industrial waste-waters.

In all cases, the oxygen concentration drops abruptly at the beginning of the measurement, but it gradually returns to the saturation value as the amount of organic matter in the biomass chamber disappears. Thus, by monitoring the oxygen concentration over time it is possible to estimate the biomass concentration, provided that we know the kinetics of the reaction. We will come back to this later on, as it is one of the main assumptions of the model, and is likely to become one of the main limitations of the physical system.

By increasing the oxygen concentration in the biomass chamber, increasing the electrolyte flow-rate also shortens the time to consume the organic matter present, and hence the analysis time. These results suggest that, by adjusting the electrolyte flow-rate and the channel length, it may be possible to ensure that there is enough oxygen in the biomass chamber to guarantee the reliability of the results. If the membrane is robust enough, we would recommend using higher flow rates (up to tens of $\mu L min^{-1}$) to ensure that oxygen is never rate limiting.

In addition to electrolyte flow-rate, we also studied the effect of channel geometry, as it will also have an impact on the amount of oxygen available, and hence in the response time of the respirometer. Figure 2 presents data at an organics initial concentration of 300 mg/l, and a flow-rate of 0.6 $\mu L min^{-1}$for h3 = 50 microns and 1.2 $\mu L min^{-1}$for h3 = 100 microns, but with a) h_1= 100 microns and h_3= 50 microns, and b) h_1=100 microns and h_3=100 microns.

Channel sizes 100 microns and greater might allow the use of less stringent filtering steps and of bigger organisms, such as yeasts.

3.3 Oxygen detection

The respirometer presented in this article monitors oxygen concentration changes in the electrolyte channel. For practical reasons, the sensor needs to be placed at the top end of the electrolyte channel, so that it does not affect the rate of the bacterial respiration. This is because since oxygen is monitored via its reduction current, which means that it is partially depleted by the working electrode. This consumption of oxygen by the electrode is normally not an issue in large-scale devices, but in this miniaturized device the effect is not negligible.

This is shown in Figure 3, where a 75 micron-wide microband is placed near the inlet of a channel of heights ranging from 50 (a) up to 150 (c) microns. The figure shows how the presence of a working electrode affects the concentration of oxygen in the channel at a given flow-rate. The figure 3 shows how as the biomass has taken the oxygen it needs. An alternative way to decrease the relative amount of oxygen consumed by the electrochemical sensor and to increase the magnitude of the measured current, is to increase the electrolyte flow-rate. [11]

channel

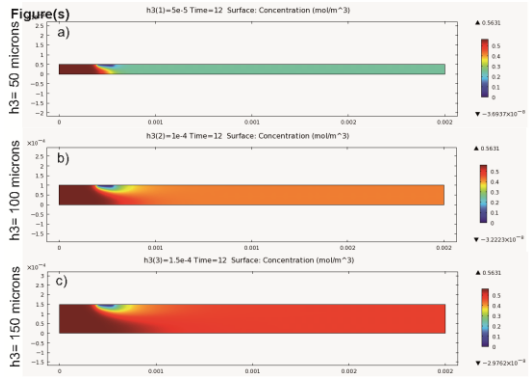

Figure 3. Electrode oxygen consumption profiles without reaction. Profiles of oxygen reduction during the amperometry process. Electrode length of 75 µm. (a) Channel of 50 µm height (h3), (b) channel of 100 µm height (h3), (c) channel of 150 µm height (h3),

Placing the sensor at the end of the electrolyte channel poses an additional advantage, as the biomass has had both more oxygen and more time available to react, and hence the oxygen concentration leaving the electrolyte channel is likely to be lower, which makes the rate of respiration easier to measure at low levels of organic matter. The curves to be analyzed must fulfill two key conditions: first, there needs to be a minimum concentration of oxygen throughout the experiment in order to prevent erroneous BOD readings. Second, the oxygen concentration drop should be sufficiently large for the data recorded by the sensor to be meaningful.

Oxygen reduction current signals will follow a typical Monod curve. First, the signal decays due to oxygen consumption of by microbes and the delay of channel recovering the inlet concentration, which is controlled by electrolyte flow-rate and oxygen diffusion across the membrane. Next, a pseudo-equilibrium establishes when the organic matter is present in excess and its degradation rate is kept more or less constant at this maximum. Last, the oxygen concentration comes back to the saturation level of oxygen once the organic matter has been consumed by the biomass. The total amount of oxygen consumed by the biomass can be easily established integrating over time the difference between the saturation concentration, which is the oxygen concentration entering the system, and the concentration measured by the sensor, until the oxygen saturation level is recovered.

This model predicts the current magnitude to range from a maximum value of 260 nA at oxygen saturation, down to about 20 nA when the oxygen concentration is at its expected minimum. These current values can be easily measured using a conventional potentiostat, so the construction of a system using the size specifications given here should be feasible.

4. Conclusions

We have designed a new concept respirometer for semi-continuous measurements of organic matter content in water samples using finite element simulations. In this system, the sample and the biomass are in a chamber on the other side of the membrane. In the presence of organic matter, the bacterial population uses oxygen as final electron acceptor, which transport rate across the membrane is key.

Oxygen transport to the biomass chamber needs to be fast to prevent the onset of anaerobic respiration and also to allow a rapid decomposition, and hence the estimation of the BOD content in the sample. The oxygen transport properties of PDMS make it a more suitable material than PTFE for the construction of respirometers when high organic loadings need to be analyzed, as thicker membranes may be used. In any case, oxygen supply may be controlled through the electrolyte flow-rate, which may in turn be used in the estimation of the BOD or of kinetic parameters related to the respiration.

The simulations presented here have yielded semi-quantitative answers before the physical device is constructed, such as (i) optimum thickness and diffusivity across membranes, (ii) effect of system geometry and flow velocities and, (iii) optimum sensor configuration. This information is extremely valuable for prototyping purposes, saving time and money, and helping to define the limits and main bottlenecks that can be expected to be found during subsequent implementation work.

Although this approach seems to allow for respiration monitoring, a real system will require the parallel use of several units such as the one described here, in order to know (i) the sensor reading of the sample in the absence of microbial population as a blank control, (ii) the basal respiration rate of the microbial population in the absence of sample or other organic matter, and

(iii) the respiration rate of the microbial population in the presence of a solution containing a known amount of organic matter, such as glucose or acetate, acting as an overall control. Additionally a study of correlation between this device results and other conventional techniques such as BOD_5 and COD must be done, to relate the results to the well-established analytical methods. Work is currently in progress to develop such a miniaturized system, which will be the subject of a separate publication.

5. References

A more exhaustive description of this work can be found at reference: Torrents et al. Bichemical Engineering Journal 66 (2012) 27-37

[1] J. Liu, B. Mattiasson, Microbial BOD sensors for wastewater analysis, Water Res. 36 (2002) 3786–3802.
[2] I. Karube, T. Matsunaga, S. Mitsuda, S. Suzuki, Microbial electrode BOD sensors, Biotechnol. Bioeng. 102 (2009) 659–672 (vintage article).
[3] O.N. Ponomareva, V.A. Arlyapov, V.A. Alferov, A.N. Reshetilov, Microbial biosensors for detection of biological oxygen demand (a review), Appl. Biochem. Microbiol. 47 (2011) 1–11.
[4] N. Godino, D. Dvila, N. Vigus, O. Ordeig, F.J. del Campo, J. Mas, F.X. Muoz, Measuring acute toxicity using a solid-state microrespirometer, Sens. Actuators B:Chem. 135 (2008) 13–20.
[5] J. Leddy, A.J. Bard, J.T. Maloy, J.M. Saveánt, Kinetics of film-coated electrodes: effect of a finite mass transfer rate of substrate across the film-solution interface at steady state, J. Electroanal. Chem. 187 (1985) 225–227.
[6] I.J. Cutress, E.J.F. Dickinson, R.G. Compton, Analysis of commercial general engineering finite element software in electrochemical simulations, J. Electroanal. Chem. 638 (2010) 76–83.
[7] R.G. Compton, A.C. Fisher, P.J. Wellington, P.J. Dobson, P.A. Leigh, Hydrodynamic voltammetry with microelectrodes – channel microband electrodes – theory and experiment, J. Phys. Chem. 97 (1993) 10410.
[8] W.B.J. Zimmerman, Multiphysics modelling with finite element methods (2006).
[9] H. Spanjers, P.A. Vanrolleghem, G. Olsson, P.L. Dold, Respirometry in control of the activated sludge process, Water Sci. Technol. 34 (1996) 117–126.
[10] J. kappeler, W. Gujer, Estimation of kinetic parameters of heterotrophic biomass under aerobic conditions and characterization of wastewater for activated sludge modelling, Water Sci. Technol. 26 (1992) 125–139.
[11] J.A. Cooper, R.G. Compton, Channel electrodes – a review, Electroanalysis 10 (1998) 141–155.

6. Acknowledgements

The authors acknowledge funding through projects Microresp (PET2008-0165-01), MEDRA (TSI020100-2011-187), Bactotox (CTQ2009-14390-C02-01 and CTQ2009-14390-C02-02) and TRAGUA (CSD2006-00044). In addition, Albert Torrents is funded by a FPU scholarship (AP2008-03848).

7. Appendix

Table 1
Model boundary conditions.

Fluid flow	Equations	Boundary
	$u = (v_0, 0)$	$x = 0, y_3 < y < y_4$
	$u = (0,0)$	$0 < x < l, y = y_3, y = y_4$
	$p = 0$	$x = l, y_3 < y < y_4$
Species transport	$O_2 = O_2{}^{sat}$	$x = 0, y_3 < y < y_4$
	$\frac{\partial O_2}{\partial y} = 0$	$0 < x < l, y = y_4$
	$\frac{\partial O_2}{\partial x} = 0$	$x = 0, y_1 < y < y_3$
		$x = 1, y_1 < y < y_3$
	$D_{O_2}^{electrolyte} \frac{\partial O_2}{\partial y}\Big\vert_{h_2^+} = \chi_f [O_2]^{electrolyte} - \chi_b [O_2]^{membrane}$	$0 < x < l, y = y_3$
	$D_{O_2}^{membrane} \frac{\partial O_2}{\partial y}\Big\vert_{h_2^-} = \chi_b [O_2]^{membrane} - \chi_f [O_2]^{electrolyte}$	$0 < x < l, y = y_3$
	$D_{O_2}^{membrane} \frac{\partial O_2}{\partial y}\Big\vert_{h_1^+} = \chi_b [O_2]^{membrane} - \chi_f [O_2]^{bioreactor}$	$0 < x < l, y = y_2$
	$D_{O_2}^{bioreactor} \frac{\partial O_2}{\partial y}\Big\vert_{h_1} = \chi_f [O_2]^{bioreactor} - \chi_b [O_2]^{membrane}$	$0 < x < l, y = y_2$
Electrode kinetics	$D_{O_2} \frac{\partial O_2}{\partial y} = k_f O_2$	$x_0 < x < x_e, y = y_4$

Table 2
Parameters and values used in the models.

Parameter	Description	Value			Units	Source
		m. effects[a]	Reaction[b]	Electrical[c]		
Geometry						
h_1	Height of reaction chamber	50	50	50–100	mm	This work
h_2	Tightness of membrane	25–75–200	25	25	10^{-6} m	This work
h_3	Height of electrolyte channel	50	50	50–100–150	10^{-6} m	This work
L	Total length	0.13	0.05	0.05	m	This work
Mass transport						
v_{in}	Mean fluid velocity	40	4–8–12–16		10^{-4} m/s	This work
T	Temperature	293.2	293.2	293.2	K	This work
Sal	Salinity	5	5	5	kg/m^3	This work
Sat	Oxygen at saturation	0.5631	0.5631	0.5631	mole/m^3	[44]
c_0_O_2_chan	Initial concentration of O_2 at channel	Sat	Sat	Sat	mole/m^3	This work
c_0_O_2_rc	Initial concentration of O_2 at reaction chamber	0	0	0	mole/m^3	This work
c_0_BOD	Initial concentration of BOD at reaction chamber	–	30–300–3,000	300	g/m^3	This work
D_{O2}_w	Diffusion coefficient of O_2 in water	3.5×10^{-9}	3.5×10^{-9}	3.5×10^{-9}	m^2/s	[45]
D_{O2}_m	Diffusion coefficient of O_2 in the membrane	3.0 PDMS	3.0 PDMS	3.0 PDMS	m^2/s	[39,40]
		0.015 PTFE	–	–		[36–38]
D_{BOD}_w	Diffusion coefficient of BOD in water	–	1×10^{-9}	1×10^{-9}	m^2/s	This work
D_{BOD}_m	Diffusion coefficient of BOD in the membrane	–	0	0	m^2/s	This work
Reactions						
bact	Bacterial concentration	–	1×10^{15}	1×10^{15}	cells/m^3	This work
$const_{bact}$	Bacterial maximum respiration rate	–	1.04167×10^{-16}	1.04167×10^{-16}	mol O_2/s	[23]
k_1	Equation XX forward constant	–	1×10^5	1×10^5	1/s	This work
k_{-1}	Equation XX backward constant	–	5×10^2	5×10^2	1/s	This work
k_2	Equation XX forward constant	–	1.25×10^6	1.25×10^6	1/s	This work
Electrical model						
c_0_R	Initial concentration of R at channel	–	–	1×10^{-7}	mole/m^3	This work
n	Number of electrons in the reaction	–	–	1		This work
E_0	Standard potential	–	–	0	V	
D_R_w	Diffusion coefficient of R in water	–	–	3.5×10^{-9}	m^2/s	
ks	Electronic transference constant	–	–	1	m/s	
α	Charge transference coefficient	–	–	0.5		
E_{eq}	Equilibrium potential, O/R	–	–	0.3926	V	
j_0	Exchange current density	–	–	2.373×10^{-5}	A/m^2	

[a] Models on membrane effects.
[b] Models with reaction.
[c] Models with reactions and electrode.